Thermal performance assessment of opaque ventilated façades for residential buildings in hot humid climates

Authors:

Research Assist. **Fulya Gökşen**, PhD. Arch.
Gazi University, Ankara, Turkey
Department of Architecture
fulyagoksen@gazi.edu.tr
Corresponding author

Prof. **İdil Ayçam**, PhD. Arch.
Gazi University, Ankara, Turkey
Department of Architecture
iaycam@gazi.edu.tr

Research Paper

Fulya Gökşen, İdil Ayçam

Thermal performance assessment of opaque ventilated façades for residential buildings in hot humid climates

In this paper, the thermal performance of opaque ventilated façades (OVFs) in the Mediterranean climate zone, where passive cooling is a priority, was examined using computational fluid dynamics (CFD). Simulations were carried out to analyse the behaviour of OVF components under different geometric configurations, using weather data for three cities in Turkey that reflect the climatic conditions of a first-degree day region. These data include the air cavity thickness, outlet size, and air cavity height. Unlike in previous literature, two-way outlet ventilation is employed in this study in the analysis of different façade systems for the Mediterranean climate region, and its performance in reducing solar gain is determined. According to the samples examined within the scope of the criteria outlined herein, it was determined that the rate of heat transferred indoors through the façade can be reduced within the range of 69 % to 75 %.

Key words:

opaque ventilated façade (OVF), computational fluid dynamics (CFD), passive cooling, residential building

Prethodno priopćenje

Fulya Gökşen, İdil Ayçam

Procjena toplinske učinkovitosti neprozirnih ventiliranih fasada za stambene zgrade u vrućim i vlažnim klimatskim područjima

U ovom je radu pomoću računalne dinamike fluida (engl. *computational fluid dynamics* - CFD) ispitana toplinska učinkovitost neprozirnih ventiliranih fasada (engl. *opaque ventilated façades* - OVF) u mediteranskoj klimatskoj zoni u kojoj je pasivno hlađenje prioritet. Simulacije su provedene kako bi se analiziralo ponašanje komponenti OVF-a pod različitim geometrijskim konfiguracijama, primjenjujući vremenske podatke za tri grada u Turskoj koji predstavljaju klimatske uvjete regije prvog stupnja-dana. Ovi podaci uključuju debljinu zračne šupljine, veličinu odvoda i visinu zračne šupljine. Za razliku od dosadašnje literature, dvosmjerna odvodna ventilacija se u ovom istraživanju primjenjuje u analizi različitih fasadnih sustava za područje mediteranske klime te se utvrđuje njezina učinkovitost u smanjenju solarnog prinosa. Prema uzorcima ispitanima u okviru ovdje navedenih kriterija, utvrđeno je da se stopa prijenosa topline u zatvorenom prostoru kroz fasadu može smanjiti za 69 % do 75 %.

Ključne riječi:

neprozirna ventilirana fasada (OVF), računalna dinamika fluida (CFD), pasivno hlađenje, stambena zgrada

1. Introduction

Currently, there is a rapid increase in the energy prices worldwide, and a decrease in the resources. Considering the climate changes and environmental pollution problems, it is essential to reduce the energy consumption in Turkey because approximately 70 % of its primary energy is obtained from foreign sources. Figure 1 shows the energy consumption rates based on the consumer type, where it can be seen that a significant share of the energy is consumed in residential buildings (26 %), [1].
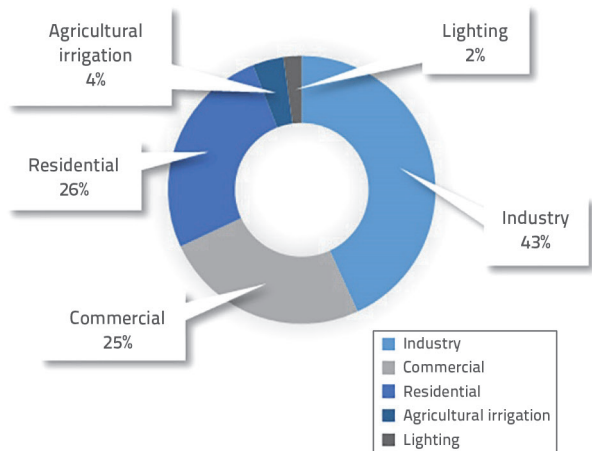

Figure 1. Turkey's Distribution of Billed Electricity Consumption in 2020 based on the Consumer Type [1]

Ispitivanja su otkrila da Turska ima veliki fond stambenih zgrada. The reviews revealed that Turkey has a high residential building stock. As shown in the graph in Figure 2, the housing stock tends to increase with each passing year [2].
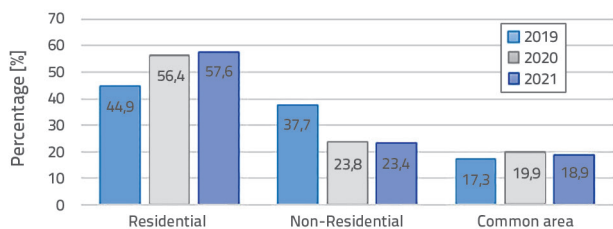

Figure 2. Rate of Increase in the Building stock in Turkey, 2019-2021 [2]

Because Turkey has different climatic zones, efforts have been made to improve the energy performance of residential buildings under the Energy Performance of Buildings Directive (EPBD) published in 2010. This is supported by the results of the review of existing academic papers, where studies on the reduction in the heating loads are more common. However, in Turkey, which has five climatic zones, the hot-humid zone accounts for 28 % of the field [3], and the energy cost for cooling buildings is higher. In residential buildings, where cost and performance optimization are priorities, the development of passive cooling techniques is important for solving envelope problems in hot zones [4, 5]. Moreover, current research has

shown that the demand for cooling in hot areas has increased by 8 % [6, 7].

For the building envelope, approximately 35 % of the heat loss [8] comes from the wall component; therefore, this component has been particularly emphasized within the scope of the research. There are many types of passive cooling strategies that can be applied to wall components in hot climates. In particular, design strategies that use ventilated façades, light façades, and sustainable materials were recently proposed.

Majority of the studies on this subject employed passive solar walls that use the ventilation caused by solar radiation to improve indoor ventilation and comfort [9, 10], double glazed façades that allow natural or mechanical ventilation for heat evacuation, [11-14] photovoltaic panels integrated into the building [15-17], and ventilated façades that have an additional layer of wall panel outside the existing façade to provide ventilation and thermal solution [18-23].

The cavity wall was first investigated by B. Vos in the Netherlands in 1963 [24, 25], who developed a system that is currently central for both the structural health and energy efficiency. It was designed to solve problems regarding the ventilation of the cavity, drain rain, and control condensation water in Northern European countries [26-29]. Recently, this system was also used in hot climates to verify its performance in reducing the cooling loads in these regions [18, 30, 31]. Currently, cavity wall systems are still in use and are regularly updated with different design solutions in different climates based on the various technological developments. Because of the research conducted in this context, ventilated façade cladding systems have been proposed.

According to the International Energy Agency (IEA), the first building with a ventilated façade was built at Cambridge University in 1967. Subsequently, ventilated façades with opaque outer layers, referred to as "opaque ventilated façades" (OVF), were used. The OVF consists of inner and external skins separated by a ventilated gap. The cladding protects against external influences such as solar radiation, water, and mechanical stress [5], and can be composed of many materials such as stone, ceramic, clay, brick, wood-based panels, precast, concrete, metal, aluminium composite, and plastic [32].

The performance of OVFs under different climatic conditions has also been investigated. Research has been conducted on the hydrothermal performance and revealed that the drying speed in VF is faster than that in non-VF [26, 28, 33]. Additionally, open-joint ventilated façade systems [30, 31, 34, 35] and the outer layer material of the façade [36-38] have been examined. The impact of wind [39-41] and effects of winter conditions on the thermal performance of façade systems have also been investigated, and different results were produced in the latter. The literature review shows that the demand for cooling energy consumption in hot regions is increasing by the day because of global warming, and the building industry should respond by adopting bio-climatic-based design strategies that employ efficient energy use. OVFs are systems that reduce the cooling

load of a building through the use of passive cooling owing to the stack effect, which due to the difference in the air density of the cavity inlet and outlet [18, 21, 22, 44, 45]. For this reason, the OVF ensures ventilation in various ways such as supporting passive cooling by acting as a solar shield, improving the indoor comfort conditions, and reducing the air conditioning demand, particularly in climates where the demand for cooling is high and during the hot summer period. Additionally, the system acts as a protective body against the effects of the sun, wind and rain; and owing to the airflow between the wall layer and the façade cladding, moisture penetration and formation on the wall is prevented, and a breathing façade system can be installed. Based on this, this system is preferred in hot humid climates.

The contribution of the OVF to the energy efficiency of buildings during the summer period has been evaluated in various studies, and its performance varies depending on the local climate (such as solar radiation, wind speed, direction, temperature) and architectural constraints (such as geometry, orientation, material). In this study, a two-way outlet vent is recommended for the OVF design. Subsequently, the difference in the details and validity of the one-way variant of the system used in existing literature were analysed for the Mediterranean climate region, and the optimum ventilation gap dimensions for the OVF system and its effect of on passive cooling in residential buildings with a high energy consumption rate were analysed. For this reason, three cities (Adana, Hatay, and Izmir) that are representative of the climatic conditions of Turkey's first-degree day zone, where the need for passive cooling is high, are referenced. Consequently, parallel, and consistent analysis results of the three pilot cities was obtained. Additionally, Adana province had the highest average value among the three cities; therefore, its climatic data was used for the design analysis.

2. Methodology

In this study, the performance of the OVF was tested using an analysis system. The most preferred programs in scientific studies involving OVF systems are the Fluent module of CFD software [21, 30, 34, 35, 40], Star CCM module of CFD software [38], TRNFlow module of TRNSYS software [43], COMSOL [42], and ESPr [46]. Among these, the ANSYS flow module of the CFD software yields the most realistic results. A comparison of the experimental and CFD results, which were used to solve similar problems, suggests that the average error rate is less than 10 % according to the experimental data, particularly when heat transfer through the ground radiation is included in the system in the simulation model [30, 40]. Therefore, the Ansys Fluent module (version: 2019-R3) of the computational fluid dynamics (CFD) software was selected because of its complex airflow and power to solve problems related to heat transfer, which are important for the investigation of the OVF performance. Figure 3 shows the flowchart for the study.
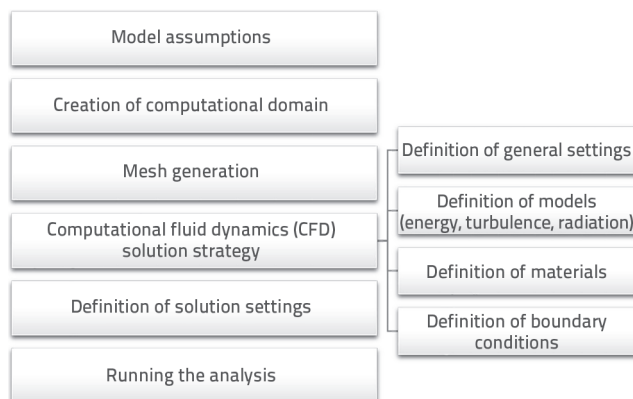

Figure 3. Flowchart showing the Ansys Fluent-CFD Analyses applied in this study

2.1. Model Assumptions

Layers of OVFs: Table 1 and Figure 4 show the dimensions and thermo-physical properties of the layers used in the façade.

Table 1. Dimensions and thermo-physical properties of the materials to be used in the OVF [47]

Facade systems F1 and F2				
Layers	Thickness [m]	Heat capacity Cp [J/(kg K)]	Density ρ [kg/m³]	Thermal conductivity λ [W/m K]
Hollow brick	0.190	781	700	0.36
Insulation (rock wool)	0.040	1030	100	0.038
Air cavity	d		Incompressible ideal gas	
Clay cladding	0.040	814	792	0.5

*Emissivity, ε = 0.9 is usually appropriate for internal and external surfaces [48].

The proposed OVF system is shown in Figure 4; where *d* is the horizontal width of the air cavity of the OVF, *de* is the OVF air cavity outlet vent size, and *H* is the height of the air cavity. In the analysis, the air cavity thickness ranges from *d* = 0.025 m to 0.25 m according to the performance standards of the Window and Cladding Technology Centre, wherein the minimum air gap istance in OVF system applications is 0.025 m, [49]. For this reason, the width of the air cavity *d* in the analysis was initiated at this rate. In addition, equal and near-equal measurements were selected when testing the dimensions of *d* and d_e using the information obtained from literature [50]. A clay-based material was preferred in this study for façade cladding because it is made from locally-sourced natural raw materials, breathable, and resistant to external weather

conditions. Moreover, it is an easily-accessible and economical material that can maintain comfortable temperatures owing to its thermal mass.
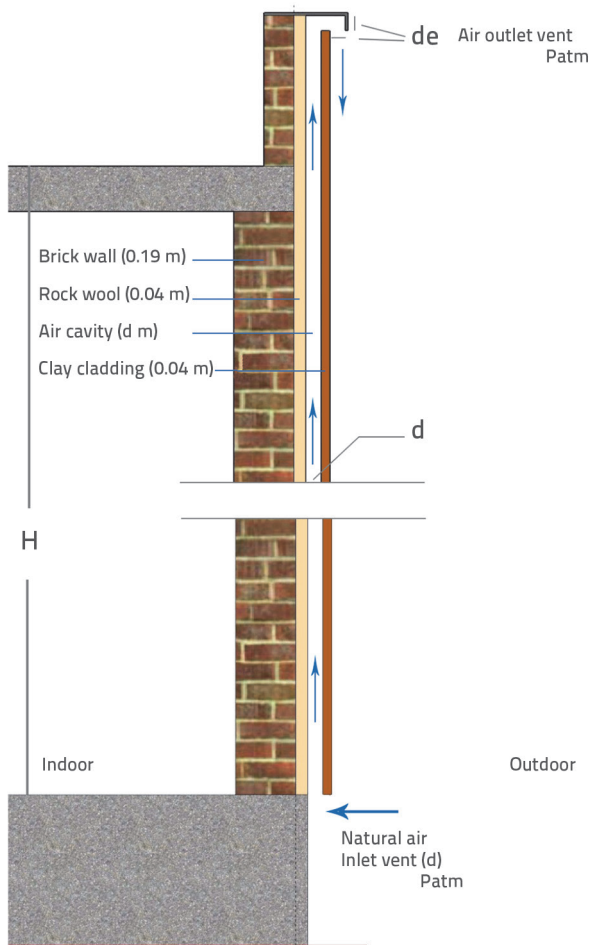

Figure 4. Cross-section of the OVF

2.2. Computational domain for the OVF

The analysis was performed to investigate how various system properties such as heat transfer between layers and vertical air movement along the air cavity of the OVF function. The first phase of the CFD analysis method involves defining a simplified geometry wherein the fluid phenomenon will be studied. In this context, the model examples in literature were examined and a proposal suitable for the scope of this study was developed [30, 40, 51, 52].

The model in Figure 5, which shows a cross-section of the OVF and the area covering its immediate surroundings, simulates the airflow in front of the façade, and is drawn in 2D on the XY coordinate plane of the ANSYS design modelling program. The OVF is positioned on the lower left corner, and the air inlet and outlet boundaries are shown in Figure 5.
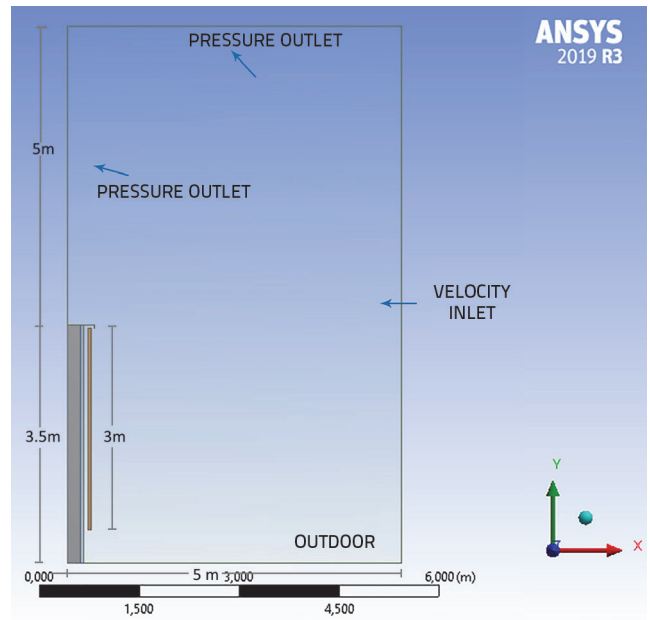

Figure 5. Computational domain for the OVF in ANSYS Fluent (produced by the author)

2.3. Mesh generation

Solving differential equations using numerical methods requires computational grids, often called meshes. A computational grid consists of the decomposition of a problem domain into basic surfaces [22]. In this study, a mesh structure was created to perform numerical solutions using the finite volume method. This section describes the properties of the selected computational grids. The mesh in the calculation domain constitutes triangular elements owing to its ability to produce geometrical dimensions (Figure 6). Therefore, meshes comprising triangular elements should be defined based on the "skewness" value, which should be on the lower side of the 0-1 range, and the maximum skewness should be < 0.8 [53].
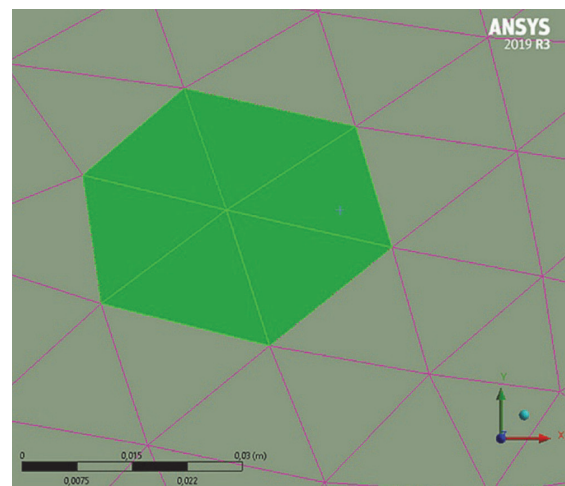

Figure 6. 2D Triangular cells of the OVF in ANSYS Fluent

The dimensions of the elements was chosen by performing a preliminary mesh-independence study. Six different numerical meshes were created, and the dependence of the numerical mesh was tested based on the obtained data. Moreover, assuming that the best mesh structure has a variability of 0.4 % or less, were used where the results converged.

Consequently, a mapped grid comprising 536.997 cells was generated over the geometry (Figure 7). First, the locations of the highest or lowest fluid property changes in both momentum and thermal relative were predicted. Accordingly, the smallest elements (0.001 m) were used at the boundaries of the cavity, and a numerical mesh system was designed to account for the physical changes that occur due to the incremental increase on the internal wall, external surface of the façade cladding, outer surfaces of the parapet wall, cap (0.002 m), and remaining surfaces of the solution volume (maximum was 0.02 m).

The quality values for the numerical mesh system are given below:
- Number of total elements: 536.997
- Maximum skewness value: 0,74481
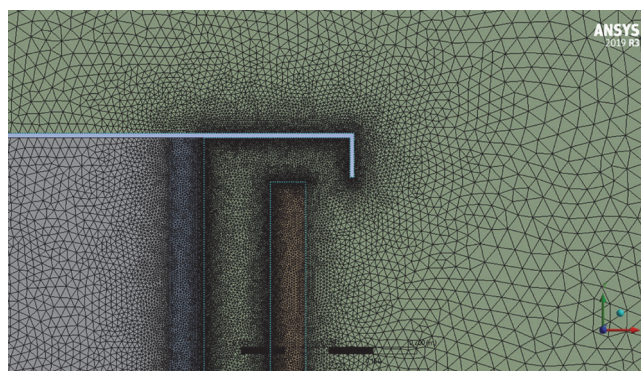- Maximum element quality: 1,0000
- Maximum aspect ratio: 3,436.

Figure 7. Mesh Model of the OVF

2.4. Solution strategy

The turbulence was modelled using a standard low Reynolds number k-epsilon turbulence model because it is suitable for natural convection flows and is preferred in literature [21, 54-56]. Moreover, because sudden changes in velocity occur in the parts of the boundary layer close to the wall, "enhanced wall treatment" was applied to the ventilated façade system because of the need for frequent meshing and high-precision resolution at the surfaces of the air cavities and outer layers. Additionally, the Y-plus value was also considered.

For the radiation Model, one of the most important features to consider when simulating ventilated façades is the solar radiation absorbed by the facade. In this context, the incident solar radiation, which has been simulated using the discrete ordinate (DO) model previous studies, was modelled as an internal heat source on the outside of the façade cladding, which is a method commonly-used in literature studies to represent the absorbed solar radiation [57]. The simulation model was based on previous studies by Sanjuan et al. [56-58]. Moreover, the DO radiation model allows can provide solutions for semi-transparent walls surface-to-surface radiation problems [59]. The solver type was selected based on the pressure, and was used to determine whether the equations will be solved collectively or separately. This parameter is preferred if the density is not decisive in the analysis study [60]. Since an ideal non-compressible gas was used in the study, an insignificant density change was expected; therefore, the analyses were carried out on a pressure basis.

2.5. Boundary conditions

In the analysis scenario, the monthly average values of the temperature, wind speed, and solar radiation intensity for July were fixed and applied to the ventilated façade model, and analyses were conducted in the steady state based on previous studies [21].

Additionally, the following physical parameters were considered for the calculation: energy model, incompressible flow, atmospheric pressure (101325 Pa), and gravity (g = 9.81 m/s^2). To describe the solar radiation incident on the outside of the façade cladding, the façade cladding was modelled as an internal heat source, and this value was used as the absorbed radiation. Moreover, the radiation and convection toward the room was considered on only the inner wall, and the heat convection coefficient was 8 W/m^2 [56].

The other boundary condition information are shown below in Figure 8, where T_0 represents the outdoor air temperature, T_e represents the outer surface temperature of the façade cladding, T_{room} represents the indoor air temperature areas residential areas (19 °C) [47], T_i represents the indoor surface temperature of the brick wall, and P_{atm} represents the atmospheric pressure (101325 P_a).
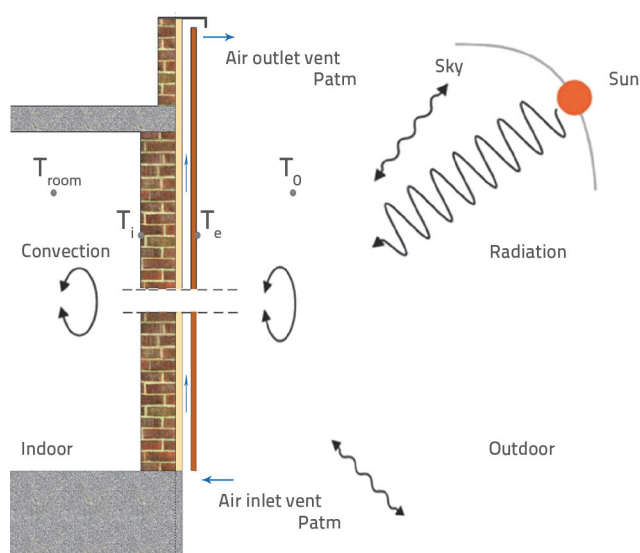

Figure 8. Boundary conditions for the OVF

In this study, the provinces in the first-degree day zone of the hot humid climate region of Turkey were examined. Ready-made climatic data were obtained using epw (EnergyPlus Weather) and based on the typical meteorological year (TMYx) extension used by EnergyPlus. The information obtained from the literature reveals that the solar radiation intensity and wind speed are decisive parameters in passive cooling [18, 19, 22, 34, 61]. In this context, the wind speed, temperature, and solar radiation values were selected based on the climatic data for July, which characterized the period requiring cooling in the selection of pilot provinces. Izmir, Hatay and Adana provinces were selected as pilot provinces owing to the following: Izmir has the highest solar radiation, wind speed, and temperature; Hatay has a low solar radiation and temperature, and high wind speed; and Adana has high solar radiation and temperature values. Additionally, analysis was done based on the data for the southern façade, where the cooling requirement is high.

Table 2. Daily temperature, radiation, and wind speed data for the cities during the summer period [62-64]

Reference province (1st July)	Solar radiation (solar radiation perpendicular to the south façade) [W/m²]	Temperature [°C]	Wind speed [m/s]
Adana	495.80	34	2.8
Hatay	490.49	31	3.1
Izmir	504.89	36	3.6

Table 3. Scenarios and combination of all parameters for the analysis of the OVF

Investigation of the optimum geometric dimension of OVFs in hot-humid climate regions							
Scenario 1 Effect of climatic data			Scenario 2 Effect of the air cavity size d and de		Scenario 3 Effect of the air cavity height	Scenario 4 Effect of the outlet direction (two-way)	
Provinces	d [m]	de [m] fix	d [m]	de [m]	H [m]	Repeat Scenario 2	
						d [m]	de [m]
Izmir	0.025	0.05	0.025	0.025	3	0.025	0.025
	0.05			0.05	6		0.05
	0.075			0.075	9		0.075
	0.10			0.10	12		0.10
	0.15		0.05	0.025	15	0.05	0.025
	0.20			0.05	18		0.05
	0.25			0.075			0.075
Adana	0.025	0.05		0.10			0.10
	0.05		0.075	0.025		0.075	0.025
	0.075			0.05			0.05
	0.10			0.075			0.075
	0.15			0.10			0.10
	0.20		0.1	0.025		0.1	0.025
	0.25			0.05			0.05
Hatay	0.025	0.05		0.075			0.075
	0.05			0.10			0.10
	0.075		0.15	0.025		0.15	0.025
	0.10			0.05			0.05
	0.15			0.075			0.075
	0.20			0.10			0.10
	0.25		0.2	0.025		0.2	0.025
				0.05			0.05
				0.075			0.075
				0.10			0.10
			0.25	0.025		0.25	0.025
				0.05			0.05
				0.075			0.075
				0.10			0.10

Subsequently, a representative case was selected to highlight the qualitative analysis of the thermal and fluid-dynamic phenomena in the façades [34, 61]. The conditions for this case correspond to summer conditions, and the solar radiation is perpendicular to the surface with a south orientation at 12.00. The climatic data for the solution domain is shown in Table 2.

3. CFD Numerical simulation results and discussion

To evaluate the performance of the parameters affecting the OVF, 88 analyses were performed. The four main titles discussed in the evaluation of the OVF system and combinations of all parameters for the analysis are given in Table 3. The aim of the analyses was to obtain an optimum OVF design and the energy quantity required for passive cooling. The most important criterion in the results is the "total heat transfer rate (W)". For this reason, comparisons were particularly made on this parameter and temperature in the scenarios.

3.1. Scenario 1: Effect of climatic data

In this section, the effects of climatic parameters such as the temperature, solar radiation, and wind speed on the air gap thickness are examined. Climatic data for Adana, Izmir, and Hatay provinces were used for analysis (Table 2). The air gap thickness in these analyses was changed and the results were compared using heat transfer and temperature graphs.

Consequently, the properties of the analysed façade and the boundary conditions are given in Table 1, Figures 4, and 8. Additionally, the wind and solar radiation are perpendicular to the south façade, and a height and depth of 3 m and 2 m, respectively, were assumed; thus, the trials were conducted on a total area of 6 m^2.
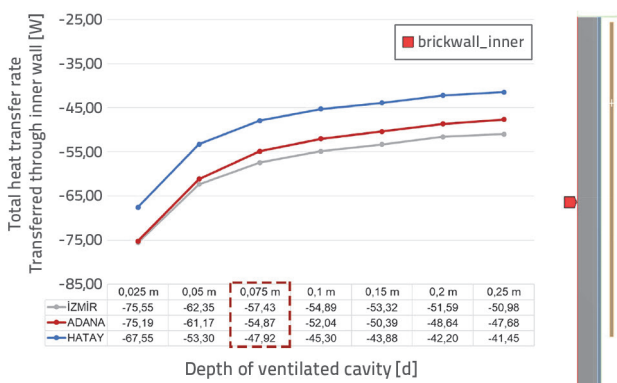

Figure 9. Heat transfer graph for Adana, Izmir and Hatay Provinces

According to the climatic data in Table 2, Izmir has higher solar radiation (504.9 W/m^2), wind speed (3.6 m/s), and temperature (35 °C) values than other provinces. Moreover, although the radiation differences between Izmir-Adana and Adana-Hatay are the same, the heat transfer results are different. Izmir

reached the same cooling level as Adana and decreased to almost the same temperature level owing to the high wind speeds that provided additional cooling. However, because the gap width increases, the velocity decreases and the difference starts increasing (Figures 9 and 10).
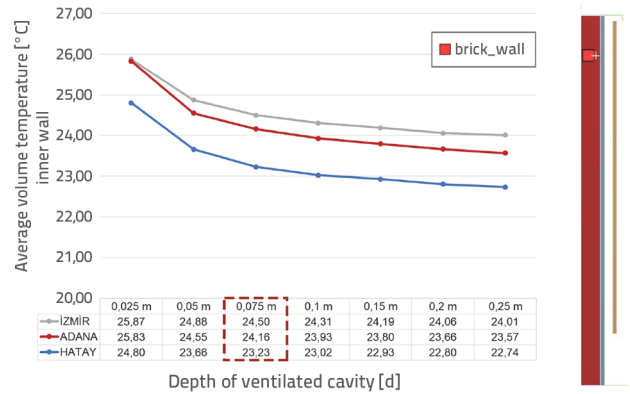

Figure 10. Temperature graph for Adana, Izmir and Hatay Provinces

The effect of the increased velocity in the ventilation gap is more evident in the comparison of Izmir with the other provinces. The air in the cavity increases because it absorbs heat from the cladding and wall. Therefore, heat transfer to the interior decreases in proportion to the waiting time of air as the waiting time in the gap decreases. Consequently, a high wind speed promotes airflow in the cavity resulting in a lower heat transfer. The graphs show that the results for the different gap dimensions in the three pilot provinces are parallel and consistent. For this reason, the climatic data for Adana province was used in the analysis of other scenarios because it has the closest value to the average among the three provinces.

3.2. Scenario 2: Effect of the air cavity size *d* and *de*

In this section, the effect of the gap thickness *d* and air outlet vent *de* on the OVF is examined. Under the same climatic conditions, all combinations were analysed, the gap thickness *d* was taken in the range of 0.025 m to 0.25 m, and the air outlet vent in the range of 0.025 m to 0.10 m. Subsequently, the results were compared based on heat transfer to indoor and temperature data. The properties of the analysed façade and the boundary conditions are given in Table 1, and Figures 4 and 8. A height and depth of 3 m and 2 m, respectively, are assumed; hence, the total trial area is 6 m^2. Additionally, the wind and solar radiation are perpendicular to the south façade.

In this scenario, the effect of the cavity thickness (*d*) on the total heat transfer rate through the inner wall is first examined. The size *d* is considered in the range of 0.025 m to 0.25 m, and based on the graph (Figure 11), it can be seen that the size and the heat transfer are inversely proportional. Additionally, the effect of the gap width was examined based on the temperature graph. Figure 12 shows a that there is a 2 °C temperature difference between the initial value and cavity width of 0.075 m, where the temperature difference starts stabilize.
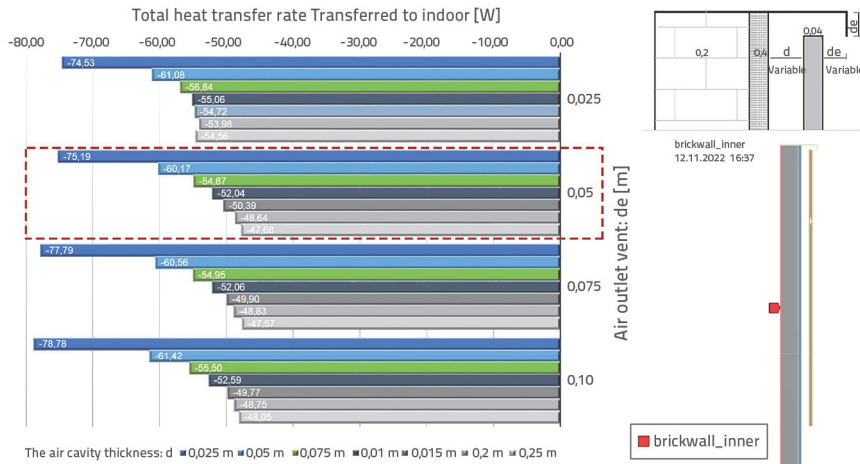
Figure 11. Analysis results for different OVF geometric configurations using heat transfer data

If there is a temperature gradient in a system, energy flows from a region with a higher temperature to a region with a lower temperature. The cladding partially absorbs the solar radiation and increases its temperature, and some of the stored energy is remitted as thermal radiation to the outdoor environment and internal wall. Moreover, an increase in the cavity width directly affects both the construction complexity and cost of the application, and the change in the air gap thickness directly affects the heat transfer; thus d is the most significant parameter during OVF design.

Analyses were conducted using de dimensions ranging from 0.025 m to 0.10 m to examine the effect of the air outlet vent size. Based on the results, a narrower de dimension increases the air velocity at the outlet vent, thereby promoting turbulence which makes it difficult to evacuate the air in this area. Additionally, the heat transferred indoors tends to increase for air outlet vents wider than 0.05 m (Figure 11).

An air gap thickness d of 0.075 m was also employed, and the dimension de was investigated. Based on analysed heat transfer results (Figure 11), the lowest ratio occurs at a $de = 0.05$ m because air is more regularly exported from the ventilation gap in this gap dimension, which causes less heat to be transferred indoors. For all these reasons, $d = 0.075$ m and $de = 0,05$ m were accepted as the optimum dimensions.
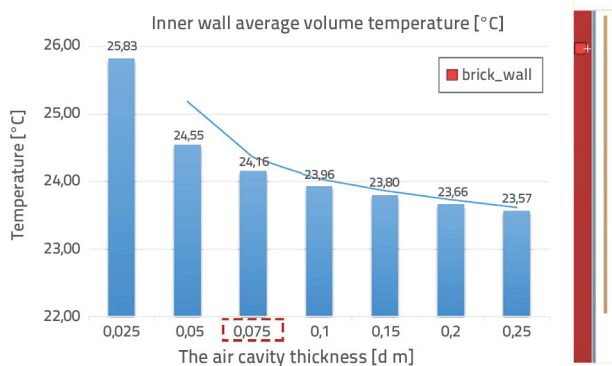

Figure 12. Effect of the air cavity thickness on the temperature

3.3. Scenario 3: Effect of the air cavity height H

In this section, different OVF heights were analysed: 3 m, 6 m, 9 m, 12 m, 15 m, and 18 m. The height was limited to 18 m because different design parameters are required to prevent the vertical spread of fire after 18-20 m [49]. Additionally, the façade has the same climatic conditions and gap dimensions as in the other scenarios, a depth of 2 m, and only the height is taken as variable. The properties of the analysed façade and the boundary conditions are given in Table 1, and Figures 4 and 8, where it was assumed that the wind and solar radiation are perpendicular to the south façade. As observed in Figure 13 and 14, as the height of the façade increases, both the wind speed and stack effect are promoted in the ventilation gap.
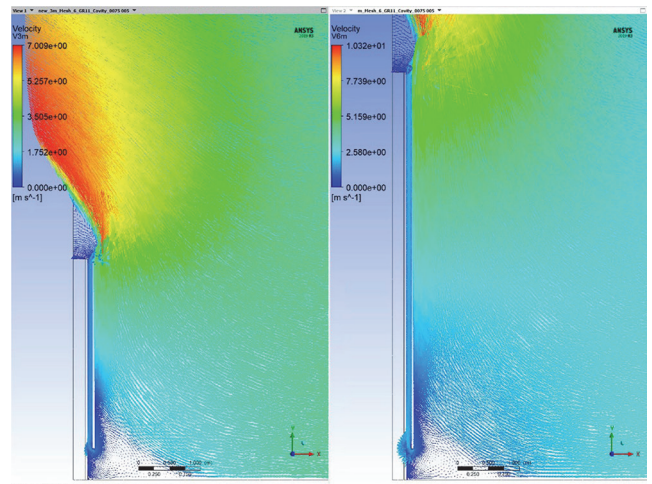

Figure 13. Relationship between the façade height and velocity gradient (H = 3 m and 6 m)

It can be seen that the increase in the wind speed in the ventilation gap directly affects the temperature and lowers the average surface temperature of the cladding (Figure 15.c). Additionally, the heat transfer to the interior is reduced in the inner layers of the façade (Figure 15.a). However, the heat transfer per square meter is slightly reduced from 0.01 to 0.001 %. Additionally, the average volume temperature of the brick walls increases by 0.3 % to 0.01 °C (Fig. 15. b).

As the air in the gap receives heat from the surfaces, its density decreases and rises, indicating that an increase in the OVF air inlet and outlet distances causes an increase in the temperature gradient with the height. Consequently, the upper components of the façade are warmer (Figure 16), resulting in a small increase in surface temperatures and close results instead of a decrease in the heat transfer.
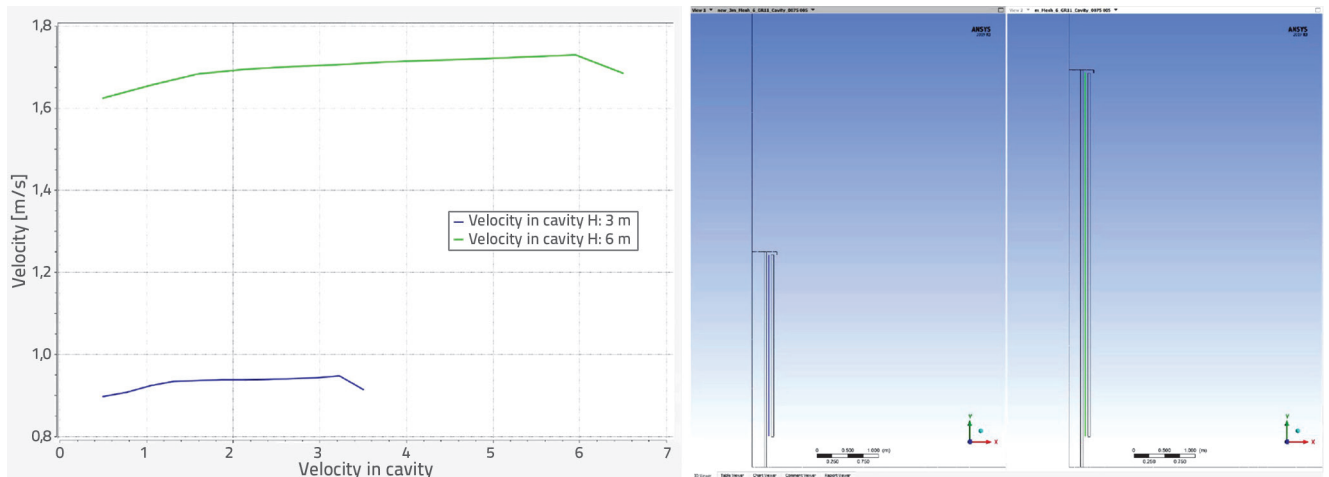
Figure 14. Relationship between the façades height and cavity velocity (H = 3 m and 6 m)

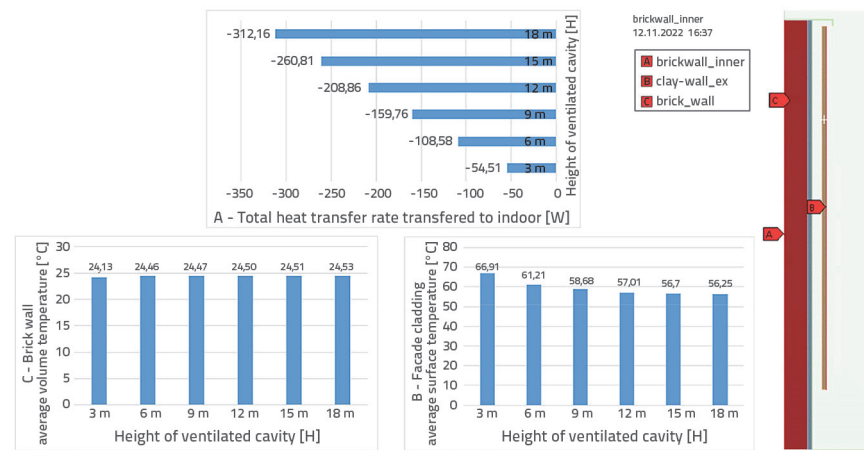Figure 15. Analysis results for the air cavity height H

Figure 16. Relationship between the façade height and temperature gradient (H = 3 m and 6 m)

3.4. Scenario 4: Effect of the outlet direction

Finally, an OVF with two air outlets was proposed as a new alternative. The optimum values of the dimensions *d* and *de* for this façade were re-examined under the same climatic conditions,

where all combinations of the F2 façade were analysed, the gap thickness *d* was selected in the range of 0.025 m - 0.25 m, and the air outlet vents are in the range of 0.025 m - 0.10 m. The results were then compared based on heat transfer indoors and temperature data.

Table 1 and Figure 17 show the properties of the analysed façades and boundary conditions. An assumed to height and depth of 3 m and 2 m are used, respectively, resulting in a total trial area of 6 m². Additionally, the wind and solar radiation are perpendicular to the south façade.
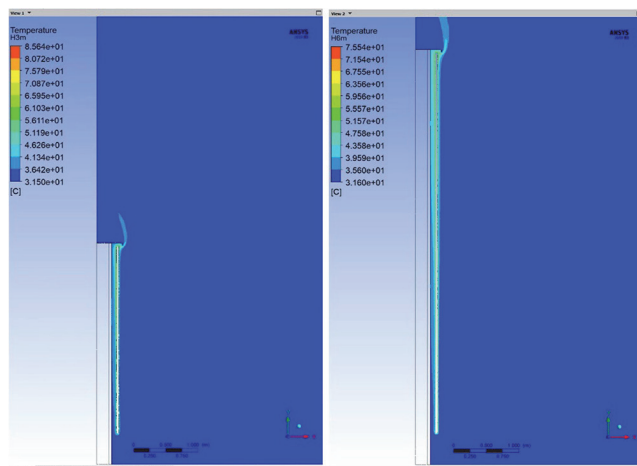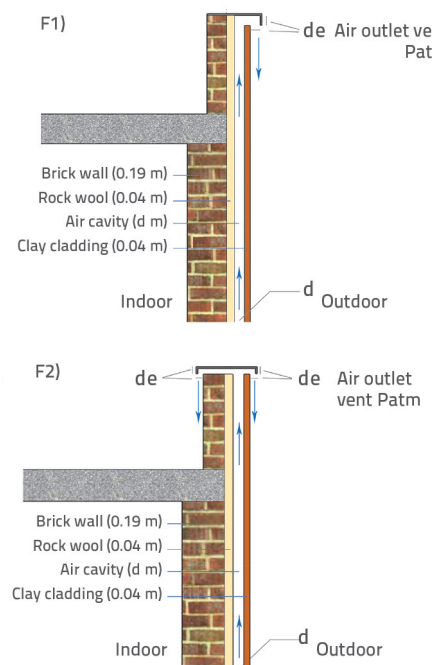

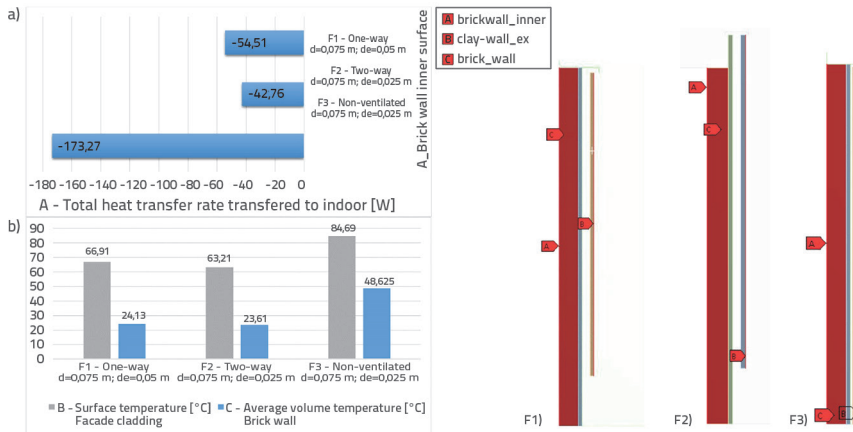Figure 17. Cross-section of the F1 and F2 façades

Figure 18. Analysis results for the F1, F2 and F3 façade systems

results of the one-way (F1), two-way (F2), and unventilated (F3) façades.

The same scenarios as those in the F1 façade were applied to determine the optimum gap dimensions of the F2 and F3 façades. Based on the results, the cavity thickness in the proposed F2 system is 0.075 m and the air outlet vents have an optimum gap size of 0.025 m.

Figure 18 shows the graphs based on the heat transfer and temperature data, and Figure 20 shows the temperature gradient. The following conclusions were drawn from the analyses of the F1, F2, and F3 façade systems with optimum dimensions.

Analyses on the thermal performance of the unventilated façade (UF) is performed followed by a comparison of the

- From Figure 18.a, the rate of heat transferred to indoor spaces when the same dimensions of the F1, F2, and F3
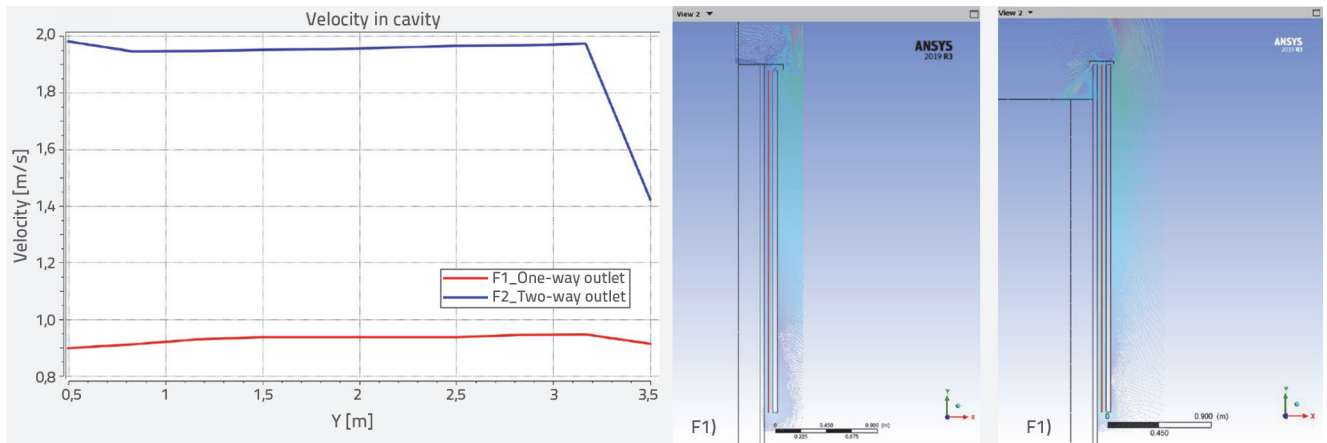

Figure 19. Velocity chart for thecavity and velocity gadient of the F1 and F2 façades
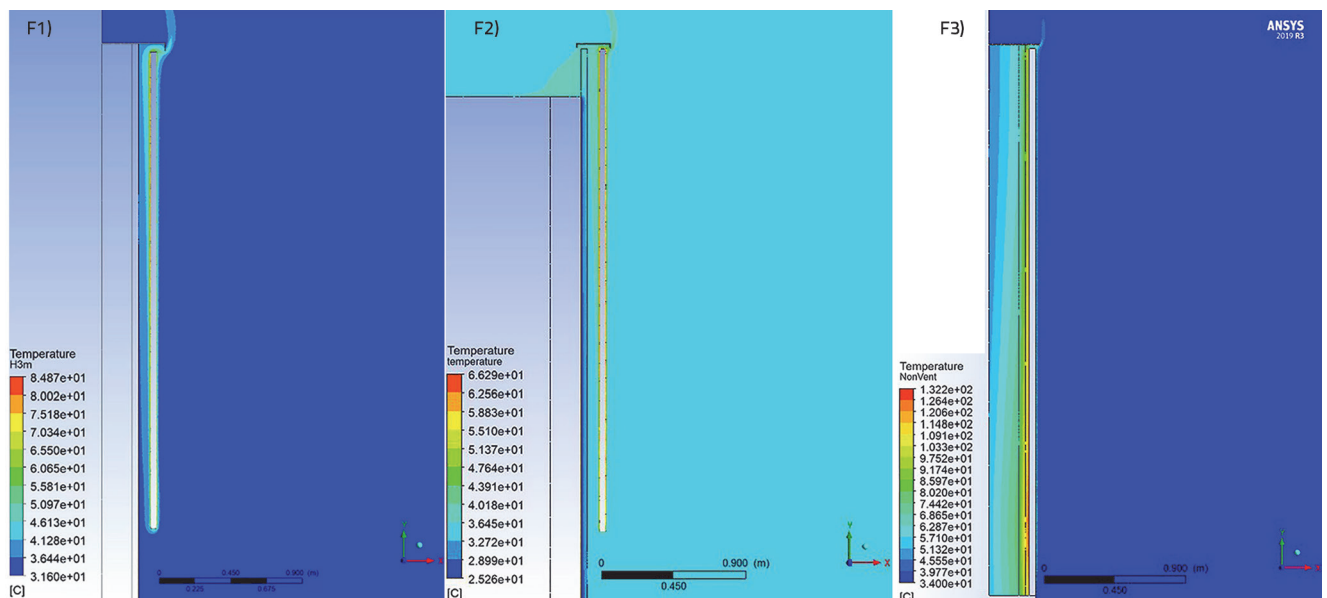

Figure 20. Temperature gradient for the F1, F2, and F3 façades

systems are used is 54,51 W, 42.76 W, and 173,27 W. That is, under the same conditions, the heat transferred to the interior can be reduced by 69 % and 75 %, respectively, in the unventilated façade.

- Moreover, based on their optimum values, the F2 system was found to transmit approximately 22 % less heat than the F1 system.
- Based on their optimum sizes, the F1 and F2 systems have almost similar values for the inner wall temperature (Figure 18.b). However, it can be seen in Figure 18.b that the façade cladding surface temperature is much lower in the F2 system, because the average velocity of the gap in the F2 system is faster than that of F1.
- According to the velocity profile in Figure 19, it can been observed that the F2 system promotes the stack effect owing to the two-way air outlet, thereby providing a rapid exchange of air in the cavity. All these results are evidence that the F2 façade system is more efficient.

As shown in Figure 20, the façade layer temperatures are very high because the façade stores heat from solar radiation and transfers it to the interior when there is no airflow,.

According to these results, ensuring controlled airflow within the building façade contributes to the provision of passive cooling.

4. Conclusion

In this study, research was conducted to investigate the OVF's ability to reduce the cooling thermal loads and optimum the size of the ventilation gaps to provide passive cooling in a hot-humid climate zone in Turkey. Analyses were conducted based on a computational fluid dynamics (CFD) approach using the FLUENT software.

The effect of climatic parameters such as temperature, solar radiation, and wind speed on the OVF was investigated. Consequently, it was revealed that the wind speed is a significant parameter affecting the thermal performance of a façade.

For the effect of the geometric configurations, the change in the air gap thickness d was found to directly affect the heat transfer; thus, it is the most significant parameter during OVF design. Moreover, increasing the cavity width directly affects both the construction complexity and cost of application. For all these reasons, a thickness of d 0.075 m was found to be the optimum value.

Additionally, a narrower de dimension increases the air velocity at the outlet, thereby promoting turbulence in this area and making it difficult to evacuate the air in the cavity. The heat transferred to the indoor tends to increase for air outlet vents wider than 0.05 m. However, the change in the size doesn't significantly affect the heat transfer. Therefore, it is not a decisive design parameter for analysis.

Moreover, the façade height increases the airflow inside the air cavity, which directly affects the temperatures. In particular, it lowers the average surface temperature of the cladding. As the air in the gap absorbs heat from the surfaces, its density decreases and rises. This means that if the OVF air inlet and outlet distances increase, the temperature gradient increases with the height, and the upper components of the façade become warmer. Therefore, a small increase in surface temperatures is observed and close results are obtained instead of a decrease in heat transfer.

For the effect of the outlet direction, the F2 system was found to promote the stack effect owing to its two-way air outlet, which facilitates a rapid exchange of air in the cavity. For this reason, the F2 façade has a lower heat transfer to the indoor space compared with the F1 façade, which has the same conditions and geometric dimensions. All these findings are evidence that the F2 façade system is more efficient than F1.

The results of this study show that compared with the unventilated F3 façade, the heat transferred to the indoor space in the one-way air outlet F1 façade and two-way air outlet F2 façade can be reduced by 69 % and 75 %, respectively.

The outcomes of this study highlight the advantages of OVF in preventing overheating during the summer period. This is because passive cooling can be achieved in areas located in hot-humid climatic zones through controlled airflow using building façades l. In future studies, the façades performance during winter and cost of the façade system should also be discussed.

REFERENCES

[1] EPDK: Enerji Piyasası Düzenleme Kurumu, 2021.

[2] TUIK: TÜİK Kurumsal, https://data.tuik.gov.tr/Bulten/Index?p=Yapi-Izin-Istatistikleri-Ocak-Eylul, -2021-37463, 11/20/2021.

[3] Türk Coğrafya Kurumu: Bölgeler ve Iller, Türk Coğrafya Kurumu, (2006)

[4] Goldsmith, N.: Building skin, Fabric Architecture, 18 (2006) 3, pp. 14-15, https://doi.org/10.1007/978-3-7643-7729-8_1.

[5] Knaack, U., Koenders, E.: Building Physics of the Envelope, De Gruyter, Berlin, 2018.

[6] IEA: World Energy Statistics and Balances (database), www.iea.org/statistics., 07/12/2021.

[7] Green Building Council: 2020 Global Status Report for Buildings and Construction, Nairobi, 2020.

[8] McMullan, R.: Environmental Science in Building, The Macmillan Press Ltd, London, 1983.

[9] Sakonidou, E.P., Karapantsios, T.D., Balouktsis, A.I., Chassapis, D.: Modeling of the optimum tilt of a solar chimney for maximum air flow, Solar Energy, 82 (2008) 1, pp. 80-94, https://doi.org/10.1016/j.solener.2007.03.001.

[10] Zamora, B., Kaiser, A.S.: Numerical study on mixed buoyancy-wind driving induced flow in a solar chimney for building ventilation, Renewable Energy, 35 (2010) 9, pp. 2080-2088, https://doi.org/10.1016/j.renene.2010.02.009.

[11] Chan, A.L.S., Chow, T.T., Fong, K.F., Lin, Z.: Investigation on energy performance of double skin façade in Hong Kong, Energy and Buildings, 41 (2009) 11, pp. 1135-1142, https://doi.org/10.1016/j.enbuild.2009.05.012.

[12] Faggembauu, D.: Heat transfer and fluid-dynamics in double and single skin facades, (2007) pp. 210,

[13] Gratia, E., De Herde, A.: Guidelines for improving natural daytime ventilation in an office building with a double-skin facade, Solar Energy, 81 (2007) 4, pp. 435-448, https://doi.org/10.1016/j.solener.2006.08.006.

[14] Saelens, D., Roels, S., Hens, H.: Strategies to improve the energy performance of multiple-skin facades, Building and Environment, 43 (2008) 4, pp. 638-650, https://doi.org/10.1016/j.buildenv.2006.06.024.

[15] Cerón, I., Caamaño-Martín, E., Neila, F.J.: State-of-the-art of building integrated photovoltaic products, Renewable Energy, 58 (2013) pp. 127-133, https://doi.org/10.1016/j.renene.2013.02.013.

[16] Quesada, G., Rousse, D., Dutil, Y., Badache, M., Hallé, S.: A comprehensive review of solar facades. Transparent and translucent solar facades, Renewable and Sustainable Energy Reviews, 16 (2012) 5, pp. 2643-2651, https://doi.org/10.1016/j.rser.2012.02.059.

[17] Zogou, O., Stapountzis, H.: Experimental validation of an improved concept of building integrated photovoltaic panels, Renewable Energy, 36 (2011) 12, pp. 3488-3498, https://doi.org/10.1016/j.renene.2011.05.034.

[18] Ciampi, M., Leccese, F., Tuoni, G.: Ventilated facades energy performance in summer cooling of buildings, Solar Energy, 75 (2003) 6, pp. 491-502, https://doi.org/10.1016/j.solener.2003.09.010.

[19] Ibañez-Puy, M., Vidaurre-Arbizu, M., Sacristán-Fernández, J.A., Martín-Gómez, C.: Opaque Ventilated Façades: Thermal and energy performance review, Renewable and Sustainable Energy Reviews, 79 (2017) April 2016, pp. 180-191, https://doi.org/10.1016/j.rser.2017.05.059.

[20] Balocco, C.: A simple model to study ventilated facades energy performance, Energy and Buildings, 34 (2002) 5, pp. 469-475, https://doi.org/10.1016/S0378-7788(01)00130-X.

[21] Patania, F., Gagliano, A., Nocera, F., Ferlito, A., Galesi, A.: Thermofluid-dynamic analysis of ventilated facades, Energy and Buildings, 42 (2010) 7, pp. 1148-1155, https://doi.org/10.1016/j.enbuild.2010.02.006.

[22] Gagliano, A., Patania, F., Ferlito, A., Nocera, F., Galesi, A.: Computational Fluid Dynamic Simulations of Natural Convection in Ventilated Facades (Chapter), Evaporation, Condensation and Heat transfer, Dr. Amimul Ahsan (Ed.), InTech, pp. 582, 2011.

[23] Gagliano, A., Aneli, S.: Analysis of the energy performance of an Opaque Ventilated Façade under winter and summer weather conditions, Solar Energy, 205 (2020) June, pp. 531-544, https://doi.org/10.1016/j.solener.2020.05.078.

[24] Vos, B.H.: Thermal and Hygric Properties of Cavity Walls(in Dutch), Technisch-Wetenschappelijk Tijdschrift, 32 (1963) 6,

[25] Hens, H., Janssens, A., Depraetere, W., Carmeliet, J., Lecompte, J.: Brick cavity walls: A performance analysis based on measurements and simulations, Journal of Building Physics, 31 (2007) 2, pp. 95-124, https://doi.org/10.1177/1744259107082685.

[26] Davidovic, D., Piñon, J., Burnett, E.F.P., Srebric, J.: Analytical procedures for estimating airflow rates in ventilated, screened wall systems (VSWS), Building and Environment, 47 (2012) 1, pp. 126-137, https://doi.org/10.1016/j.buildenv.2011.04.002.

[27] Falk, J., Molnár, M., Larsson, O.: Investigation of a simple approach to predict rainscreen wall ventilation rates for hygrothermal simulation purposes, Building and Environment, 73 (2014), pp. 88-96, https://doi.org/10.1016/J.BUILDENV.2013.11.025.

[28] Falk, J., Sandin, K.: Ventilated rainscreen cladding: A study of the ventilation drying process, Building and Environment, 60 (2013), pp. 173-184, https://doi.org/10.1016/J.BUILDENV.2012.11.015.

[29] Suresh Kumar, K.: Pressure equalization of rainscreen walls: A critical review, Building and Environment, 35 (2000) 2, pp. 161-179, https://doi.org/10.1016/S0360-1323(99)00015-3.

[30] Giancola, E., Sanjuan, C., Blanco, E., Heras, M.R.: Experimental assessment and modelling of the performance of an open joint ventilated façade during actual operating conditions in Mediterranean climate, Energy and Buildings, 54 (2012), pp. 363-375, https://doi.org/10.1016/j.enbuild.2012.07.035.

[31] Marinosci, C., Semprini, G., Morini, G.L.: Experimental analysis of the summer thermal performances of a naturally ventilated rainscreen façade building, Energy and Buildings, 72 (2014), pp. 280-287, https://doi.org/10.1016/j.enbuild.2013.12.044.

[32] Romalia, C.: General principles for the design and construction of ventilated facades, Universitatea Tehnică „Gheorghe Asachi" din Iași Tomul LIX (LXIII), 10 (2013) 3, pp. 161-169,

[33] Davidovic, D., Srebric, J., Burnett, E.F.P.: Modeling convective drying of ventilated wall chambers in building enclosures, International Journal of Thermal Sciences, 45 (2006) 2, pp. 180-189, https://doi.org/10.1016/j.ijthermalsci.2005.06.002.

[34] Suárez, M.J., Sanjuan, C., Gutiérrez, A.J., Pistono, J., Blanco, E.: Energy evaluation of an horizontal open joint ventilated faade, Applied Thermal Engineering, 37 (2012), pp. 302-313, https://doi.org/10.1016/j.applthermaleng.2011.11.034.

[35] Sanjuan, C., Sánchez, M.N., Heras, M. del R., Blanco, E.: Experimental analysis of natural convection in open joint ventilated façades with 2D PIV, Building and Environment, 46 (2011) 11, pp. 2314-2325, https://doi.org/10.1016/j.buildenv.2011.05.014.

[36] Stazi, F., Vegliò, A., Di Perna, C.: Experimental assessment of a zinc-titanium ventilated façade in a Mediterranean climate, Energy and Buildings, 69 (2014), pp. 525-534, https://doi.org/10.1016/j.enbuild.2013.11.043.

[37] Stazi, F., Tomassoni, F., Vegliò, A., Di Perna, C.: Experimental evaluation of ventilated walls with an external clay cladding, Renewable Energy, 36 (2011) 12, pp. 3373-3385, https://doi.org/10.1016/j.renene.2011.05.016.

[38] Labat, M., Woloszyn, M., Garnier, G., Rusaouen, G., Roux, J.J.: Impact of direct solar irradiance on heat transfer behind an open-jointed ventilated cladding: Experimental and numerical investigations, Solar Energy, 86 (2012) 9, pp. 2549-2560, https://doi.org/10.1016/j.solener.2012.05.030.

[39] Mora-Pérez, M., López-Patiño, G., Amparo López-Jiménez, P.: Quantification of Ventilated Façade Effect Due to Convection in Buildings Buoyancy and Wind Driven Effect, Researches and Applications in Mechanical Engineering, 3 (2014)

[40] Gagliano, A., Nocera, F., Aneli, S.: Thermodynamic analysis of ventilated façades under different wind conditions in summer period, Energy and Buildings, 122 (2016), pp. 131-139, https://doi.org/10.1016/j.enbuild.2016.04.035.

[41] Naboni, E., Tarantino, S.: The Climate Based Design of Opaque Ventilated Façades, Energy Forum Bressanone, (2014) Naboni, pp. 1023-1030,

[42] Guillén, I., Gómez-Lozano, V., Fran, J.M., López-Jiménez, P.A.: Thermal behavior analysis of different multilayer façade: Numerical model versus experimental prototype, Energy and Buildings, 79 (2014), pp. 184-190, https://doi.org/10.1016/j.enbuild.2014.05.006.

[43] Aparicio-Fernández, C., Vivancos, J.L., Ferrer-Gisbert, P., Royo-Pastor, R.: Energy performance of a ventilated façade by simulation with experimental validation, Applied Thermal Engineering, 66 (2014) 1-2, pp. 563-570, https://doi.org/10.1016/j.applthermaleng.2014.02.041.

[44] Gregório-Atem, C., Aparicio-Fernández, C., Coch, H., Vivancos, J.L.: Opaque ventilated façade (OVF) thermal performance simulation for office buildings in Brazil, Sustainability (Switzerland), 12 (2020) 18, https://doi.org/10.3390/su12187635.

[45] Looman, R.: Climate-responsive design: A framework for an energy concept design-decision support tool for architects using principles of climate-responsive design, A+BE Architecture and the Built Environment, 1 (2017), pp. 1-282,

[46] Marinosci, C., Strachan, P.A., Semprini, G., Morini, G.L.: Empirical validation and modelling of a naturally ventilated rainscreen façade building, Energy and Buildings, 43 (2011) 4, pp. 853-863, https://doi.org/10.1016/J.ENBUILD.2010.12.005.

[47] TS 825: Binalarda Isı Yalıtım Kuralları. Türk Standartları Enstitüsü, Ankara, 2013.

[48] EN ISO 6946:2017: Building components and building elements - Thermal resistance and thermal transmittance - Calculation methods, Dublin, Ireland, 2017.

[49] CWCT: Centre for Window & Cladding Technology, https://www.cwct.co.uk/pages/facets#!articles/1222-9011-0204-drained-and-ventilate, 10/17/2021.

[50] Šagát, E., Matějka, L., Pěnčík, J.: Experimental Assessment of the Influence of Outlet Geometry on the Airflow and Temperatures in the Ventilated Façade Cavity, Applied Mechanics and Materials, 824 (2016), pp. 641-648, https://doi.org/10.4028/www.scientific.net/amm.824.641.

[51] Nghana, B., Tariku, F., Bitsuamlak, G.: Assessing ventilation cavity design impact on the energy performance of rainscreen wall assemblies: A CFD study, Building and Environment, 196 (2021) March, pp. 107789, https://doi.org/10.1016/j.buildenv.2021.107789.

[52] Lerma, C., Mas, Á., Gil, E., Vercher, J.: Hygrothermal Behaviour of Continuous Air Chambers on Stone Panels Façades through CFD and IRT, Applied Sciences, 9 (2019) 15, pp. 3001, https://doi.org/10.3390/app9153001.

[53] ANSYS: ANSYS FLUENT 12.0 User's Guide - 6.2.2 Mesh Quality, https://www.afs.enea.it/project/neptunius/docs/fluent/html/ug/node167.htm, 10/18/2021.

[54] Chen, Q.: Comparison of different k-ε models for indoor air flow computations, Numerical Heat Transfer, Part B: Fundamentals, 28 (1995) 3, pp. 353-369, https://doi.org/10.1080/10407799508928838.

[55] Xamán, J., Álvarez, G., Lira, L., Estrada, C.: Numerical study of heat transfer by laminar and turbulent natural convection in tall cavities of façade elements, Energy and Buildings, 37 (2005) 7, pp. 787-794, https://doi.org/10.1016/j.enbuild.2004.11.001.

[56] Sanjuan, C., Suárez, M. J., González, M., Pistono, J., Blanco, E.: Energy performance of an open-joint ventilated façade compared with a conventional sealed cavity façade, Solar Energy, 85 (2011) 9, pp. 1851-1863, https://doi.org/10.1016/j.solener.2011.04.028.

[57] Sanjuan, C., Suárez, M.J., Blanco, E., Heras, M.D.R.: Development and experimental validation of a simulation model for open joint ventilated façades, Energy and Buildings, 43 (2011) 12, pp. 3446-3456, https://doi.org/10.1016/j.enbuild.2011.09.005.

[58] Sanjuan, C.: Análisis Del Comportamiento Térmico Y Fluido-Dinámico De Las Fachadas Ventiladas De Junta Abierta, Universidad de Oviedo, Madrid.

[59] FLUENT, A.: 12.0 Theory Guide, 2009.

[60] ANSYS FLUENT 13 User's Guide: Ansys Fluent Theory Guide, 2013.

[61] Santa Cruz Astorqui, J., Porras-Amores, C.: Ventilated Façade with double chamber and flow control device, Energy and Buildings, 149 (2017), pp. 471-482, https://doi.org/10.1016/j.enbuild.2017.04.063.

[62] NOAA: Solar Calculator Links, https://gml.noaa.gov/grad/solcalc/sollinks.html, 01/18/2022.

[63] EPW: Climatewebsite\WMO_Region_6_Europe\TUR_Turkey, https://climate.onebuilding.org/WMO_Region_6_Europe/TUR_Turkey/index.html, 01/12/2022.

[64] European Commission: JRC Photovoltaic Geographical Information System (PVGIS) - European Commission, https://re.jrc.ec.europa.eu/pvg_tools/en/tools.html#PVP, 04/05/2022.